SCIENTIFIC Publishing Limited

**New Energy Exploitation and Application**

https://ojs.ukscip.com/index.php/neea

*Article*

# Energetic Viability of a Dense Plasma Focus-Based Fusion-Fission Hybrid Reactor: Gas-Cooled Fast Reactor Concept

**Jorge A. García Gallardo**

Bariloche Atomic Centre, National Atomic Energy Commission (CNEA), Bariloche CP 8400, Argentina

* Correspondence: jorge.gallardo@cab.cnea.gov.ar; Tel.: +54-9-294-444-5100

**Received:** 22 April 2025; **Revised:** 18 May 2025; **Accepted:** 20 May 2025; **Published:** 5 June 2025

**Abstract:** The Fusion-Fission Hybrid Reactor (FFHR) is a sort of reactor that generates energy through a subcritical set, using neutrons produced in a nuclear fusion device. The viability of such a reactor has already been studied by many authors. One of the most challenging problems to solve is that the energy generated by fission is usually insufficient to feed the fusion device, but this could be addressed by using a Dense Plasma Focus (DPF) as a neutron source in conjunction with the so-called Multiplying Cascade (MC), which is a concentric arrangement of the fuel elements. The DPF is a very cheap and simple device that acts as a pulsed neutron source and seems to be promising in the future nuclear industry. The use of composite materials like cermets as fuel can improve energy efficiency by raising the operational temperature of the core. Also, a blanket of FLiBe, which is a molten salt, can provide the required amount of tritium by using the outgoing neutron flux. Because of the fast spectrum of this device, the use of gas as a coolant becomes convenient. In this way, the FFHR becomes a Gas-cooled Fast Reactor (GFR), allowing it to combine high temperature and fast spectrum. It is possible to find a function of energy that indicates under what conditions the reactor can run. As the system includes fusion and fission in the same device, it inherits from both processes the concepts of criticality and break-even at the same time.

**Keywords:** Fusion-Fission Hybrid Reactor; Dense Plasma Focus; Cermet; FLiBe; Gas-cooled Fast Reactor

## 1. Introduction

Despite continued efforts in research, pure nuclear fusion reactors are still far from becoming a reality. In such reactors, the nuclear fuel, deuterium (D-D) or deuterium-tritium (D-T), is heated to such a temperature that it becomes plasma, a state of matter consisting of ions, electrons, and perhaps some neutral atoms. Eventually this plasma will produce nuclear fusion reactions. For a device of this type to work, the amount of energy obtained by nuclear fusion must at least be equal to the energy invested in heating and confining the plasma, a condition known as break-even. Keeping the plasma confined at the proper temperature and density long enough to reach the break-even point represents a big challenge not yet achieved. However, a nuclear fusion device can generate abundant neutrons to feed a subcritical fission set. This arrangement is called a Fusion-Fission Hybrid Reactor (FFHR). In such a reactor, as the fusion device becomes just a neutron source, the operating requirements for the fusion device are much easier to achieve than the break-even of a pure fusion reactor.

Subcritical means that the fission arrangement can only be powered by an external neutron source, as its neutron multiplying parameter, $k_{eff}$, will always be $k_{eff} < 1$, so the system is inherently safe, and no control rods are needed [1,2]. Furthermore, hybrid reactors, in general, would produce fast spectra that could be used to burn undesirable isotopes [3–7].

The first problem to solve in the FFHR is to ensure that the fusion device provides the neutrons at a reasonable energy cost so that the total balance is favorable. Some proposals consider that this goal could be achieved if the fusion device is a Dense Plasma Focus (DPF). A DPF is a simple device that consists of two concentric electrodes housing the fusion fuel, usually D-D or D-T. By establishing a potential difference between both electrodes, the DPF forms a sheet of plasma. This sheet accelerates axially until it collapses at the other end of the device. Then, the plasma is violently compressed into a small packet called a pinch, reaching such a temperature and density that it can produce many neutrons [8]. Although it is not entirely clear, it is believed that most of those neutrons come from a beam-target nuclear fusion reaction, and a small part is generated by thermonuclear fusion [8,9]. Anyway, these devices can produce nuclear fusion reactions in small volumes with an energy efficiency not achieved by any other device, and then, they produce a high neutron yield per input energy [10–13]. In addition, these devices are so small and cheap that it is very tempting to use them as neutron sources. For instance, they don't have coils, and the use of easily activating materials like copper can be minimized.

Nevertheless, if the DPF is filled with D-T, it will produce 14 MeV neutrons, which is a very high energy for the subcritical set. In addition, its yield would not be enough to drive the system. These problems could be solved if the fission fuel were divided into two concentric fuel shells (FS) with a big void between them. This configuration will profit from the reflection of the neutrons between the shells, increasing the probability that each neutron will produce a fission reaction and transforming the 14 MeV peak into a more convenient spectrum. This arrangement is called a Multiplying Cascade (MC) and was proposed previously by many authors [13–16].

In an FFHR, thermal-to-electrical conversion is always required, since the fusion device, whatever it may be, requires electrical energy to run. Then, the thermal-electrical conversion efficiency plays a key role in the synergy of the system. Higher efficiencies require increasing the temperature of operation. In addition, due to the fast spectrum, water must be avoided in the coolant. These requirements suggest using gas. Then, the FFHR becomes a type of gas-cooled fast reactor (GFR). The GFRs are one of the types of reactors considered as part of Gen-IV due to their advantages in combining high energy efficiency and nuclear waste minimization [17,18].

On the other hand, the use of combined cycles and modern tungsten alloy turbines would allow efficiencies above 60%, which will increase the temperature of operation (above 1300 K) [19–23]. This goal can be achieved by using the so-called cermets, that is, fuels made of ceramic + metal composite materials, particularly tungsten and uranium dioxide, whose operational limit temperatures are close to 3000 K [24]. Cermets date back to the 1960s when, in the framework of the space race, fuels with the ability to withstand high temperatures began to be studied, since only in this way would future Nuclear Thermal Propulsion (NTP) be efficient. Furthermore, due to their expected reliability, the cermets were even proposed in the construction of nuclear jet engines. More recently, new space travel projects have also renewed interest in cermets [24–28].

As the fusion device uses D-T for its operation, the supply of tritium becomes relevant. Then, a layer of breeder blanket is necessary. Such material is usually lithium titanate or silicate, given its high lithium concentration per volume [29–31]. However, these materials typically decompose near 1200 K in such a way that in a high-temperature reactor environment, they will lose their structural properties [32]. A solution to this problem may come from the molten salts. Among the molten salts recommended for this task is the combination of LiF + $BeF_2$, known as FLiBe. The FLiBe was originally intended to operate in Molten Salt Reactors (MSR), and then, it was also evaluated to work in the environment of a fusion reactor [33–35].

## 2. Materials and Methods

This work analyzes a reactor formed with a subcritical set made of Cermet W/46U(50)O2. This cermet is the most used one for high-temperature purposes. W/46U(50)O2 means tungsten with 46% of 50%-enriched uranium dioxide, and 46% refers to weight (this would be equivalent to 60% in volume) of $UO_2$ [24–26].

The dimensions were chosen to be close to those previously published under similar concepts. For example, Clause et al. proposed a reactor fitted with two spherical layers made of 8%-enriched metallic uranium and whose total external diameter is 4 meters [14]. Talebi et al. proposed a cylindrical device with 3.77%-enriched uranium for the inner layer of fuel and 0.45%-enriched uranium for the outer one, with a total diameter of around 10 meters [15]. And the reactor from Gallardo et al. is made of the fast-spectra alloys U-25Pu-10Zr and U-7Pu-10Zr and has a diameter of 9.6 meters [13]. The reactor in the present work is restricted to a total diameter of 3 meters.

Among the possible DPFs that can be used as neutron sources, there is the FF-1, designed and built by Lerner

et al. [10–12]. This is a small yet powerful device that occupies a volume of approximately one liter. The reasons for choosing this device are that it has the highest yield for its size, it is well-tested, and its concept is still in the improvement stage. The energy that feeds a DPF is initially stored in a capacitor bank, being, in this case, 60 kJ. This energy is released to the concentric electrodes of the device, discharging the capacitor. Of course, to charge the capacitor again requires a specific amount of time, making the DPF a pulsed device. In the literature, each of these pulses is often referred to as a shot.

## 2.1. The Concentric Model

An FFHR based on DPF follows the concept of a concentric model. In this model, the fusion device is in the center of many spherical shells [14,36].

The fuel is arranged to form the MC in this way: the first spherical fuel shell will be called FS1, and it surrounds the DPF, followed by a second fuel shell called FS2. Between FS1 and FS2, there is a large space. These two shells are equivalent to the core of a conventional fission reactor. The cermet W/46U(50)O2 is expected to have a good performance in this reactor due to the reflecting and multiplying properties of the tungsten in the fast neutron spectrum, as previously studied [37].

Surrounding the subcritical set is the tritium generator blanket (FLiBe), and finally, a spherical reflector shield that encloses the entire reactor. The voids between all these shells are occupied by the flowing coolant, hydrogen, or helium, usually.

## 2.2. The Fission Parameters

It is required to find the multiplication factor $k_{eff}$ of the whole system. This parameter has to fulfill the condition $k_{eff} < 1$, but as the system must be permitted to vary its $k_{eff}$, a range of possible values must be considered. The lower the value of $k_{eff}$, the further the system is from criticality, making it safer. But this will also reduce the energy obtained through fission, making it more difficult to reach the energy self-sufficiency of the system. On the contrary, a value of $k_{eff}$ very close to one would provide a good amount of energy, but it would reduce the margin of safety as the probability of the system becoming accidentally critical ($k_{eff}$ = 1) would arise. There is a lot of discussion in the bibliography about the adequate operational limits of $k_{eff}$ in the subcritical set. Many authors consider the operational point close to 0.980, so the range considered here will be between 0.975 and 0.985 [13–16].

The fission energies $\varepsilon_1$ and $\varepsilon_2$ obtained for both FS1 and FS2, respectively, are also required for each value of $k_{eff}$. There are analytical models to find approximately all these values for this sort of arrangement, but, given the complex interactions of reflection and multiplication that occur within the system, it is more accurate to do Monte Carlo simulations with MCNP5, including the high-temperature libraries ENDF66e (3000K) and ENDF5mt (800K) [13–15].

One of the most interesting properties of the MC is its geometrical capability of changing the value of $k_{eff}$ in the subcritical set by changing the radii of FS1 and FS2 without changing the total mass of fuel. This occurs because the reflective and multiplying properties of the MC depend strongly on the voids in the system. This property will be used to obtain a set of different configurations, each with different $k_{eff}$ (and then, with different fission energies) but with the same mass of fuel [14].

## 2.3. Energy Flow and Balance

As any fusion device works only with electrical energy, it is essential to take into account the conversion to study the energy balance and to find out if the whole system is self-sustaining. Also, particularly as the DPF is a pulsed device, the energy balance must be analyzed for each shot.

The diagram in **Figure 1** describes the energy flow in the system during a shot. Marked in bold, C, R, and G represent, respectively, the capacitor (where the DPF energy is stored), the reactor itself (where the fusion-fission reactions occur), and the electrical generator. On the left, there is an arrow that indicates that the system must be started with an energy $E_o$, which is what the DPF requires to work. This energy is stored in the capacitor C and is a key parameter since its value defines the number of neutrons generated by the device. Leaving C to the right, approximately half of the energy, $E_1$, returns to the capacitor C, and the rest, $E_2$, is divided into a large part, $E_s$, that is converted into thermal energy and a smaller one, $E_p$, which is used to form the pinch in the DPF.

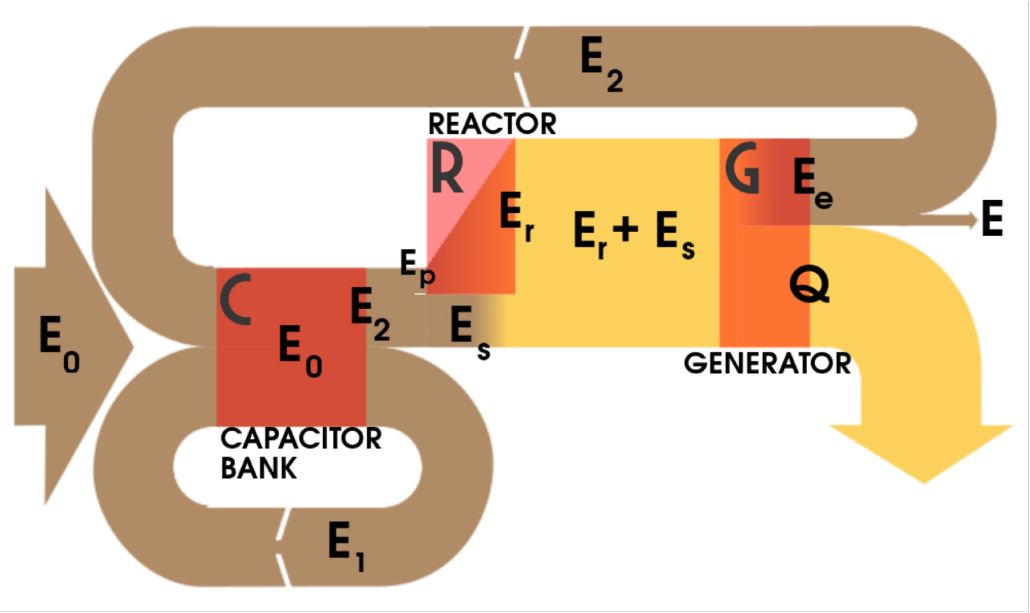


**Figure 1.** To Start the System, an Energy $E_o$ Should be Provided, as Shown by the Arrow on the left. The Sectors C, R, and G are, respectively, the DPF Capacitor, the Fusion-Fission Reactor, and the Electric Generator. At the End of the Cycle, the System Releases the Electric Energy E and Heat Q. The Brown Sectors Indicate Electric Energy, and the Yellow Ones Indicate Thermal Energy.

This $E_p$ is what generates nuclear fusion and the neutrons that use the subcritical system R to produce the thermal energy $E_r$. Both $E_r$ and $E_s$ are used to generate electrical energy in G. If we call $\eta$ the efficiency of thermal-to-electric generation, then $E_e = \eta(E_r + E_s)$, where $E_e$ is the total electrical energy produced by G, and $E_r + E_s$ is the total available thermal energy. In turn, the energy $E_p$, which is used to generate the pinch, is only a small fraction $\zeta$ of the energy $E_o$ initially in the capacitor; that is, $E_p = \zeta E_o$.

On the other hand, the energy $E_2$ that is required to be returned to the capacitor bank to trigger the DPF again is also a fraction $f$ of $E_o$; that is, $E_2 = fE_o$. Both $\zeta$ and the feedback factor $f$ depend exclusively on the DPF and are usually typical values: $\zeta = 0.07$ and $f = 0.5$ [11,38,39].

Finally, we must find the relationship between the energy $E_r$ generated by the subcritical set and the initial energy $E_o$ in the capacitor bank. If the masses of FS1 and FS2 are $m_1$ and $m_2$, respectively:

$$E_r = (\varepsilon_1 m_1 + \varepsilon_2 m_2) Y(E_o) \tag{1}$$

where $\varepsilon_1$ and $\varepsilon_2$ are the fission energies per unit mass of fuel and per neutron in the source for both shells FS1 and FS2, respectively, and $Y(E_o)$ is the neutron yield of the fusion device, which is a function of the energy $E_o$. In the case of the DPF, there is a semi-empirical rule that establishes that, for $E_o \leq 100$ kJ, the yield is $Y(E_o) = c_y E_o^2$, where $c_y$ is a parameter that depends on each particular DPF and can be found from the fitting of experimental data [8,39,40]. Therefore, replacing $Y(E_o)$ in eq. (1):

$$E_r = \alpha E_o^2 \tag{2}$$

where $\alpha = (\varepsilon_1 m_1 + \varepsilon_2 m_2) c_y$. Then, it is possible to write down the net electrical energy $E$, obtained by the device, as a function of the energy $E_o$ in the capacitor bank:

$$E = \eta \alpha E_o^2 + [\eta(f - \zeta) - f] E_o \tag{3}$$

As stated in the previous subsection, $\varepsilon_1$ and $\varepsilon_2$ depend on the $k_{eff}$ of the subcritical set, so varying $k_{eff}$ will result in parabolas with different openings.

### 2.4. The Tritium Breeder Blanket

The tritium breeder blanket is the layer where the system profits from the remaining neutrons, i.e., the neutrons that run outwards from the FS2, to produce tritium through the reactions $^{6}$Li(n, t)$^{4}$He and $^{7}$Li(n, n't)$^{4}$He, with $^{6}$Li and $^{7}$Li being the two isotopes composing natural lithium.

In a previous work by Gallardo et al., a lithium silicate was analyzed, giving a high amount of tritium. But, in this case, the high-temperature environment of the reactor would make this silicate lose its structural properties [13,31]. To avoid this problem, the proposed material here for the breeder blanket is the molten salt FLiBe, which is an eutectic made of 66% (mass proportion) of LiF and 34% of $BeF_2$. This eutectic has a density of 2.46 g/cm$^3$ when solid and 1.94 g/cm$^3$ in liquid state. Its melting point is 733 K (460 °C), meaning that the reactor should be running for the FLiBe to flow [33–35].

The advantage of having a molten salt blanket is that it enhances the extraction of tritium, and also, it would remove heat from the last layers of the reactor, thus acting as a coolant.

The amount of tritium atoms generated in the blanket by each neutron in the source and by each lithium atom in the material is called the Tritium Production Rate (TPR) and indicates the rate at which tritium atoms are produced when exposed to a neutron flux. The TPR can be obtained directly by MCNP5, and then it is possible to calculate the ratio $N_{TG}/N_{TS}$, which is the number of tritium atoms produced in the FLiBe compared to the number of tritium atoms used in the source, using the formula $N_{TG}/N_{TS} = N_{Li}$ TPR, where $N_{Li}$ is the number of lithium atoms in the blanket. This ratio is easier to read than the TPR, as $N_{TG}/N_{TS} = 1$ means that the tritium production equals the tritium expenditure; $N_{TG}/N_{TS} < 1$ means insufficient production of tritium, and $N_{TG}/N_{TS} > 1$ means that a surplus of tritium is being generated.

## 3. Results and Discussion

Experimentally, the maximum yield of the FF-1 operating with D-D is $2.5 \times 10^{11}$ neutrons per shot when $E_o$ = 60 kJ. According to the bibliography to date, this device has never been filled with D-T, but it is easy to estimate its neutron yield in such a case, as the DPF scales ×100 its yield when changing from one fuel to another in the same device and with the same conditions, according to previous experimental research. This is just a consequence of the bigger cross section for the D-T reactions keeping the same temperature and time conditions [38,39]. Therefore, a device with the same characteristics of the FF-1 operating with D-T will give $2.5 \times 10^{13}$ neutrons per shot, with the same $E_o$ = 60 kJ, meaning thus $c_y = 6.94 \times 10^{9}$ kJ$^{-2}$ [12,13].

As stated before, the operating point of the subcritical set has been established around $k_{eff}$ = 0.980, giving an operating range between 0.975 and 0.985. Then, three families of curves have been drawn by slightly varying $k_{eff}$ inside this range (see **Figure 2**). To do this, both radii of FS1 and FS2 were varied, keeping their volumes constant as explained before. The values of $\varepsilon_1$ and $\varepsilon_2$ were found by using MCNP5.

As an example, three possible values of the conversion efficiency $\eta$ are used: 0.55, 0.60, and 0.65. These values would require different degrees of improvement in the real thermal-to-electric conversion being realistic (55%), optimistic (60%), and very optimistic (65%).

In **Figure 2**, the line break-even for $E = 0$ has been drawn: below this line the reactor cannot operate, and only for values $E > 0$ is there net energy obtained. The most remarkable thing about this diagram is that the hybrid reactor has a break-even value of $E_o$, a typical concept of a fusion reactor, for each value of $k_{eff}$, a typical concept of a fission reactor. The hybrid reactor therefore inherits both concepts at the same time. The figure also shows that, to maintain the same output energy, when $k_{eff}$ changes from A to B, it is necessary to increase the input energy $E_o$.

Note the system's sensitivity to $k_{eff}$. For $\eta$ = 0.60, a small 0.6% change in $k_{eff}$, i.e., from $k_{eff}$= 0.979 to $k_{eff}$ = 0.985, results in a 67% change in the output energy $E$. On the other hand, for a fixed $k_{eff}$ = 0.979, a change in $\eta$ from 0.6 to 0.65, i.e., 8%, results in a 23% change in $E$. Of course, the variations are clearly nonlinear, and further analysis is required to assess the system's sensitivity; however, it reveals the implications that small variations in $k_{eff}$ could have.

The previous analysis was calculated for one shot; but, to get an idea about the output power of the system, an estimation of the shot frequency must be done. The time-limiting factor of the DPF is the time of charge of the capacitor bank. Frequencies of 1 Hz have been obtained with capacitors as large as 150 kJ, and with a 60 kJ capacitor, higher frequencies are expected [40]. But supposing an arrangement of ten DPF shooting synchronously at 1 Hz

each, a total frequency of 10 Hz is possible. A combination of many devices inside the inner void of the system has already been proposed previously [13,15,16]. For example, Talebi et al. propose an arrangement of four DPFs radially disposed, pointing to the center of the void. A similar configuration of ten DPFs 10 cm high and 14 cm in diameter can fit perfectly in the 90 cm diameter spherical void of the reactor analyzed in this work. From **Figure 2**, the DPF operates under reasonable conditions, which would be $Eo$ = 60 kJ, $\eta$ = 0.6, and $k_{eff}$ = 0.979. This gives E = 5 kJ per shot, meaning 50 kW output electric power (approx. 0.6 MW of total thermal power) shooting at 10 Hz. If a DPF similar to FF-1 is able to work under extreme conditions ($Eo$ = 100 kJ, $\eta$ = 0.65, and $k_{eff}$ = 0.979), the same analysis will give E = 37 kJ per shot or 370 kW of electric power (approx. 1.3 MW total thermal power). These figures are very low for a massive reactor like the one presented in this work, especially compared with the commercial operating ones. This very low power/weight ratio is a consequence of the low neutron yield of the source and the low shooting frequency: it will be necessary to somehow increase these two parameters for the reactor to have a clear application.

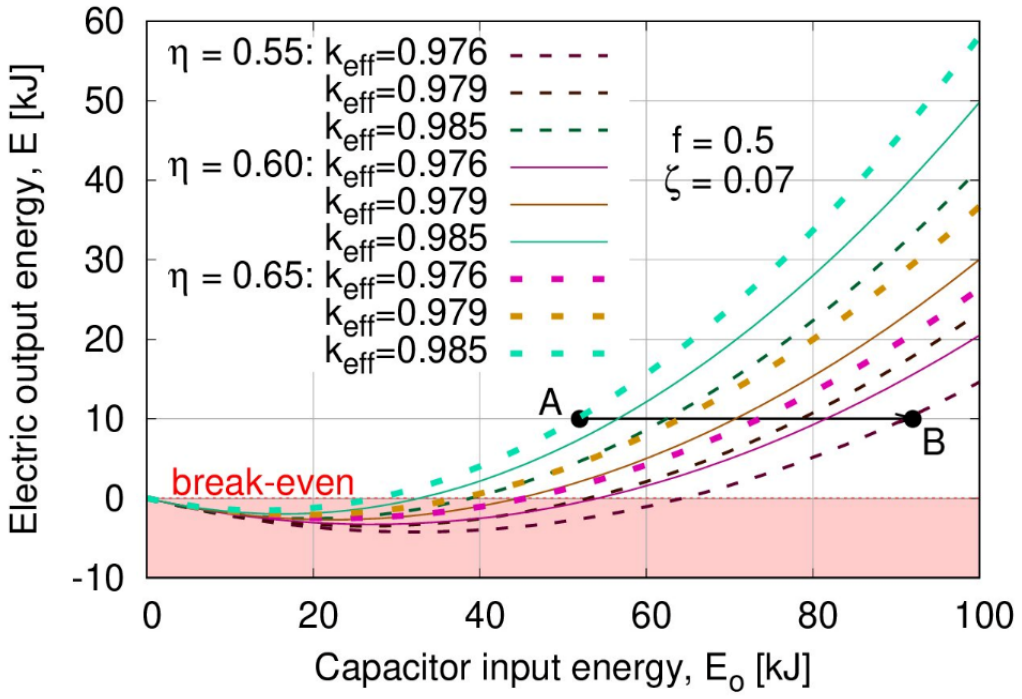


**Figure 2.** Electric Output Energy from Equation 3 Produced in the Hybrid Reactor, as a Function of the Capacitor Energy $E_o$. The $\alpha$ Factor was Obtained by Means of MCNP5 and the ENDF66e (3000K) and ENDF5mt (800K) Libraries. The Path Between Condition A and Condition B Keeps E Constant by Increasing $E_o$.

The spectra obtained from FS1, FS2, and the FLiBe are shown in **Figure 3**, where it can be seen that it is indeed a fast reactor. In the FLiBe, the neutron spectrum shows the typical peak structure of $^{19}$F close to the 0.1 MeV region [41]. The FLiBe blanket is separated inwards by a thin layer of tungsten (approx. 2 cm). The thickness of this inner layer is very important since it acts as a semi-reflector of neutrons coming from the core. Outwards from the FLiBe layer, there is the thick shell of tungsten, acting as a reflector. As can be seen in **Figure 3**, the absorption of neutrons, despite being greater than in the case of silicates (see ref. 13), is not too much to absorb too many neutrons.

**Table 1** shows the values of TPR and the ratio $N_{TG}/N_{TS}$ obtained in the system for three values of $k_{eff}$. If compared with the values obtained in solid silicates and titanates, it can be said that in this case it is considerably lower, and this is mainly due to the lower amount of lithium per blanket volume [29–31]. From the work of Gallardo et al., for instance, the ratio $N_{TG}/N_{TS}$ = 36 for its massive blanket of 300 tons [13]. Taking into account that the blanket mass in the present work is just 2.3 tons, the results of Table 1 are relatively good. Besides, for this system, the ratio $N_{TG}/N_{TS}$ is always greater than one, even for the lower $k_{eff}$, so the system would be self-sufficient in tritium supply.

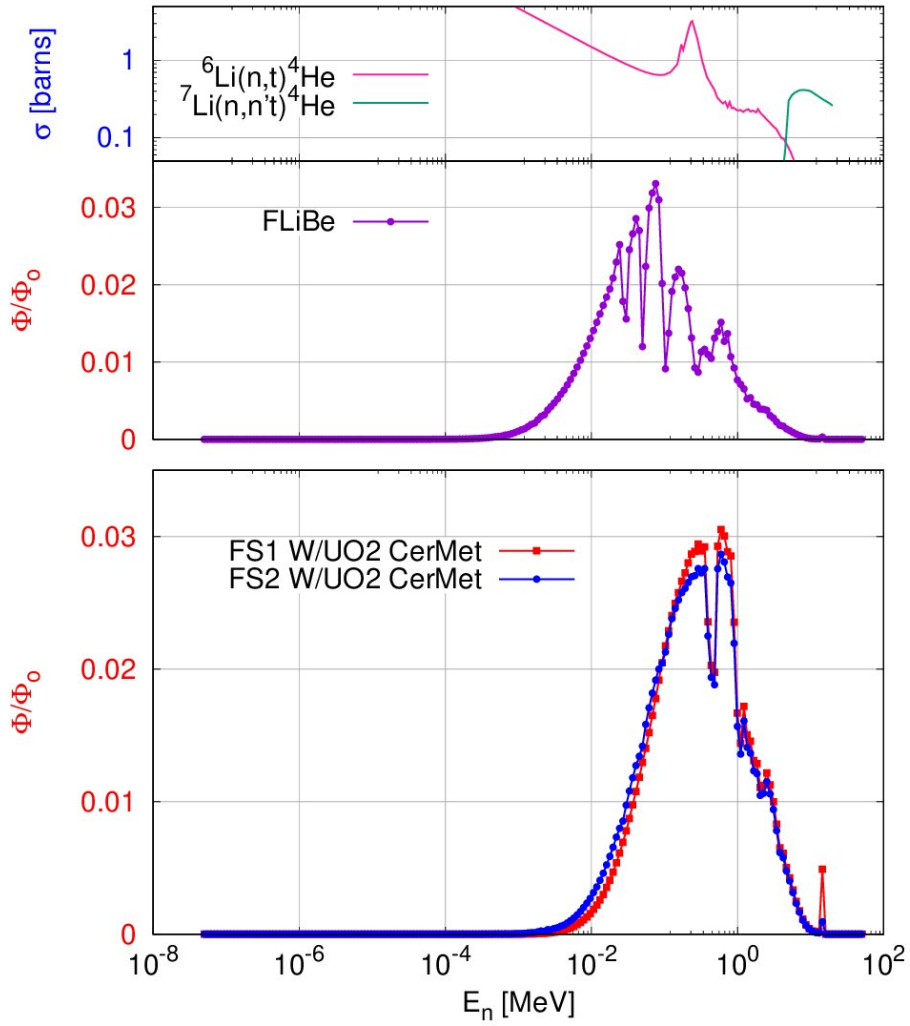


**Figure 3.** Neutron Spectra in the FLiBe and the Fuel Shells FS1 and FS2, Normalized by Total Flux $\Phi_o = \Sigma_E \Phi_E$. For Comparison Purposes, the Cross-Sections for the Reactions $^6Li(n, t)^4$He and $^7Li(n, n't)^4$He Were Added on Top [42–46].

**Table 1.** Variation of the Tritium Generation in the FLiBe Layer as a Function of the Neutron Multiplication Factor $k_{eff}$.

| $k_{eff}$ | TPR | $N_{TG}/N_{TS}$ |
|---|---|---|
| 0.976 | $3.7 \times 10^{-29}$ | 1.267 |
| 0.979 | $4.4 \times 10^{-29}$ | 1.523 |
| 0.850 | $5.9 \times 10^{-29}$ | 2.052 |

**Figure 4** shows schematically the general configuration of a possible system based on FFHR running a combined thermal cycle. According to the concentric model, the DPF arrangement is placed at the center of the void, producing neutrons that escape radially, reaching then the first fuel layer, the FS1. In FS1, a combined effect of fission, reflection, and multiplication will generate more neutrons that reach the FS2, traversing the large void between them. The fission in these two shells will generate the thermal energy that heats the helium that flows radially from the center (gray arrows). The shell FS2 also emits neutrons that were produced by fission or by multiplication in the tungsten. The neutrons that escape from FS2 outwards reach the blanket of FLiBe, covered internally by a 2 cm layer of tungsten that separates the FLiBe from helium and acts as a semi-reflector. The tritium recovery system from the irradiated FLiBe is also shown in the figure. Fluid circulation and the water/helium and helium/FLiBe

heat exchangers were also drawn, the latter acting as part of a second cooling system. Finally, the outer shell of the reactor is a 10 cm thick layer of tungsten that acts as a neutron reflector and as shielding. The general data for this reactor are summarized in **Table 2**.

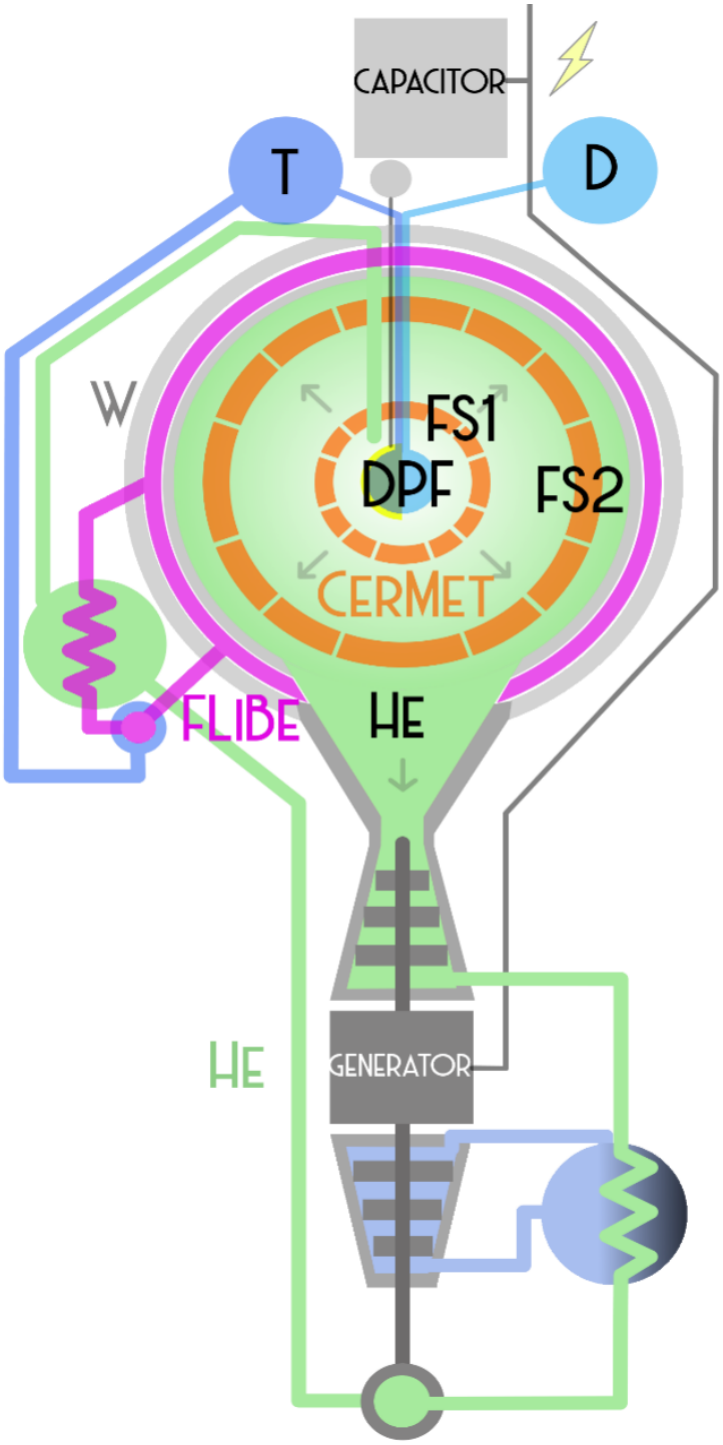


**Figure 4.** Possible Configuration of a Hybrid Reactor Based on a Cermet and Molten Salts Breeder Blanket. The FS1 and FS2 Fuel Layers Surround the Fusion Device in the Center (DPF). A Fluid Layer of FLiBe Then Captures the Outgoing Neutrons. The Helium Flows Through This System, Which Works as a Combined Cycle. The Entire Reactor is Shielded by a Layer of Tungsten.

**Table 2.** Summarized Data for the Hybrid Reactor Based on DPF and MC. The Fuel Mass in This System is Just 23% of the Total Mass.

| | | |
|---|---|---|
| **Fuel** | material<br>FS1 internal radius<br>FS1 thick<br>FS2 internal radius<br>FS2 thick<br>total mass | Cermet W/46U(50)O2<br>45 cm<br>20 cm<br>77 cm<br>38 cm<br>19 Ton. |
| **Internal Reflector** | material<br>internal radius<br>thick<br>mass | natural tungsten<br>133 cm<br>2 cm<br>9 Ton. |
| **Breeder Blanket** | material<br>internal radius<br>thick<br>mass | FLiBe<br>135 cm<br>5 cm<br>2.3 Ton. |
| **Shielding** | material<br>internal radius<br>thick<br>mass | natural tungsten<br>140 cm<br>10 cm<br>51 Ton. |
| **General Parameters** | diameter<br>mass | 3 m<br>81.3 Ton. |

## 4. Conclusions

The Fusion-Fission Hybrid Reactor has been presented as a possible step between the conventional fission reactors and the future pure fusion reactors. The configuration described here is based on the Dense Plasma Focus (DPF) and the multiplying cascade (MC) previously studied by many authors. To obtain high thermal-to-electric conversion efficiency, it is necessary to reach high temperatures, which suggests the system should become a high-temperature gas reactor. This would only be possible with suitable materials in the core, such as cermets. However, the temperatures for which the cermets were designed far exceed those that conventional gas turbines can withstand. It must be remembered at this point that cermets were developed to be used in systems where the greater proportion of the energy is converted into propulsion, such as NTP devices. So, if we want the reactor to be used to generate electric energy, it will be necessary to greatly improve the alloys of the turbines to take advantage of the high-temperature gas leaving the reactor core. On the contrary, if the thermal energy is the main output to be used, like in the case of the NTPs, the power/weight ratio must be highly improved.

As an advantage, this system would be able to electrically control the output energy, which makes the typical control rods unnecessary. Eliminating these rods is an advantage that should not be overlooked, especially in applications where the reactor should move.

One key factor to take into account in favor of the DPF device is the cost. For example, the total cost of the FF project, which includes the FF-1 and the new FF-2B (still under testing), is less than US$ 500,000 [10]. However, the DPF is a pulsed device, and the characteristic charging time of the capacitor bank (ranging from seconds to minutes) imposes a limitation on the frequency of the shots. For a DPF in the range of $E_o$ = 100 kJ, this frequency is of the order of 1 Hz. Also, a restriction to $E_o$ is imposed by the 100 kJ limit of the DPF scaling law. The only way to avoid these problems is to install many DPFs and shoot them synchronously. This does not seem to be a great difficulty, since the DPF itself is a small device, and in the internal void of the reactor, several of them could fit. For example, these DPFs could be installed radially as proposed by previous works. The capacitor bank and accessory systems could be located outside the shielding. If ten DPFs are installed, then 10 Hz is possible, allowing an electric output of a few tens of kilowatts. For any application, increasing the shooting frequency would be a great improvement in the machine's performance.

Another point to highlight is that the curves in **Figure 2** were obtained from the maximum yield of the FF-1, assuming the use of D-T. Unfortunately, that yield cannot be sustained over several shots, since, for many reasons, it decreases considerably: by taking several shots, the average yield is approximately 60% of the maximum value. Although research is still ongoing, one of the causes of this phenomenon could be found in the particles released by the electrodes. These particles could be contaminating the plasma. But even if this state-of-the-art device works at its maximum capacity, the yield would remain so low that it would require a subcritical set with a $k_{eff}$ > 0.976 to reach the break-even. From the point of view of the amount of fuel, this makes it practically indistinguishable from

a conventional critical reactor. The DPF, although a simple device, needs to be improved.

And finally, perhaps the biggest flaw in this concept is that it requires 50% enriched uranium, putting the device far beyond the 20% required to accomplish the LEU IAEA certifications, thus raising concerns about proliferation.

## Funding

This work received no external funding.

## Institutional Review Board Statement

Not applicable.

## Informed Consent Statement

Not applicable.

## Data Availability Statement

Data will be made available upon reasonable request.

## Acknowledgments

The author wants to thank M.A.N. Giménez for his kind collaboration with MCNP.

## Conflicts of Interest

The author declares no conflict of interest.

## References

1. Bethe, H. A. The Fusion Hybrid. *Phys. Today* **1979**, *32*, 44–51.
2. Nifenecker, H.; David, S.; Loiseaux, J. M.; et al. Hybrid Nuclear Reactors. *Prog. Part. Nucl. Phys.* **1999**, *43*, 683–827.
3. Acır, A.; Übeyli, M. Burning of Reactor Grade Plutonium Mixed with Thorium in a Hybrid Reactor. *J. Fusion Energy* **2007**, *26*, 293–298.
4. Şahin, S.; Şahin, H. M.; Acır, A. LIFE Hybrid Reactor as Reactor Grade Plutonium Burner. *Energy Convers. Manag.* **2012**, *63*, 44–50.
5. Şahin, S.; Şahin, H. M.; Acır, A. Utilization of Reactor Grade Plutonium as Energy Multiplier in the LIFE Engine. *Fusion Sci. Technol.* **2012**, *61*, 216–221.
6. Plukienė, R.; Plukis, A.; Juodis, L.; et al. Transmutation Considerations of LWR and RBMK Spent Nuclear Fuel by the Fusion–Fission Hybrid System. *Nucl. Eng. Des.* **2018**, *330*, 241–249.
7. Stacey, W. M.; Stewart, C. L.; Floyd, J.-P.; et al. Resolution of Fission and Fusion Technology Integration Issues: An Upgraded Design Concept for the Subcritical Advanced Burner Reactor. *Nucl. Technol.* **2014**, *187*, 15–43.
8. Lee, S.; Saw, S. H. The Plasma Focus–Numerical Experiments, Insights and Applications. In *Plasma Science and Technology for Emerging Economies*; Rawat, R. S., Ed.; Springer Nature Singapore Pte Ltd.: Singapore, 2017; pp. 113–232.
9. Scholz, M. *Plasma-Focus and Controlled Nuclear Fusion*; Institute of Nuclear Physics: Krakow, Poland, 2014.
10. Lerner, E. J.; Hassan, S. M.; Karamitsos-Zivkovic, I.; et al. Focus Fusion: Overview of Progress Towards p–B11 Fusion with the Dense Plasma Focus. *J. Fusion Energy* **2023**, *42*, 7.
11. Lerner, E. J.; Murali, S. K.; Blake, A. M.; et al. Fusion Reaction Scaling in a Mega-Amp Dense Plasma Focus. *Nukleonika* **2012**, *57*(2), 205–209.
12. Lerner, E. J.; Hassan, S. M.; Karamitsos, I.; et al. Confined Ion Energy 200 keV and Increased Fusion Yield in a DPF with Monolithic Tungsten Electrodes and Pre-Ionization. *Phys. Plasmas* **2017**, *24*, 102708.
13. García Gallardo, J. A.; Giménez, M. A. N. Self-Sustainability and Energy-Balance in a Fast Fusion–Fission Hybrid Reactor (FFHR) Based on Dense Plasma Focus (DPF) and Multiplicative Cascade. *Prog. Nucl. Energy* **2022**, *147*, 104184. [CrossRef]
14. Clausse, A.; Soto, L.; Friedli, C.; et al. Feasibility Study of a Hybrid Subcritical Fission System Driven by Plasma-Focus Fusion Neutrons. *Ann. Nucl. Energy* **2015**, *78*, 10–14.

15. Talebi, H.; Kiai, S. M. S. Conceptual Design of a Hybrid Fusion–Fission Reactor with Intrinsic Safety and Optimized Energy Productivity. *Ann. Nucl. Energy* **2017**, *105*, 106–115.
16. Kiai, S. M. S.; Talebi, H.; Adlparvar, S. A Compact Fusion–Fission Hybrid Reactor. *J. Fusion Energy* **2018**, *37*, 161–167.
17. Zohuri, B. *Generation IV Nuclear Reactors*; Elsevier: Amsterdam, Netherlands, 2020.
18. Schultz, K. R. Gas-Cooled Fusion–Fission Hybrid Reactor Systems. *J. Fusion Energy* **1981**, *1*, 163–183.
19. Barnert, H.; Kugeler, K. HTR Plus Modern Turbine Technology for Higher Efficiencies. In Proceedings of Technical Committee Meeting on Design and Development of Gas Cooled Reactors with Closed Cycle Gas Turbines, Beijing, China, 30 October–2 November 1995; pp. 67–82.
20. Strengthened Superalloy for Gas Turbine Blades. *Met. Powder Rep.* **1992**, *47*(10), 24–28. [CrossRef]
21. Schubert, W.-D. Gas Turbines for Power Plants and Mechanical Drive Applications. *Tungsten Newsletter. Tungsten in Superalloys*, March 2017, pp. 17–18. Available online: https://www.itia.info/wp-content/uploads/2023/07/ITIA_Newsletter_2017_03.pdf (accessed on 5 May 2025).
22. Yang, X.; Qu, X.; Wang, J. Combined Cycle-Coupled High-Temperature and Very High-Temperature Gas-Cooled Reactors: Part I–Cycle Optimization. *Ann. Nucl. Energy* **2019**, *134*, 193–204.
23. Kwon, H. M.; Moon, S. W.; Kim, T. S.; et al. A Study on 65% Potential Efficiency of the Gas Turbine Combined Cycle. *J. Mech. Sci. Technol.* **2019**, *33*(9), 4535–4543.
24. Bhattacharyya, S. K. An Assessment of Fuels for Nuclear Thermal Propulsion. ANL/TD/TM01-22, 12 December 2001. [CrossRef]
25. Reid, R. E.; Semple, E. L.; Simpson, J. D. Selection of 710 Reference Reactor. GEMP-514, May 1967. General Electric Co.: Cincinnati, Ohio, USA.
26. Hickman, R.; Broadway, J. *Hot Hydrogen Testing of Tungsten–Uranium Dioxide (W–$UO_2$) CERMET Fuel Materials for Nuclear Thermal Propulsion*; NASA Marshall Space Flight Center: Huntsville, AL, USA, 2010.
27. Song, J.; An, W.; Wu, Y.; et al. Neutronics and Thermal Hydraulics Analysis of a Conceptual Ultra-High Temperature MHD Cermet Fuel Core for Nuclear Electric Propulsion. *Front. Energy Res.* **2018**, *6*, 29.
28. Fan, Y.; Yan, R.; Zhu, G.; et al. Design of a Prismatic CERMET Megawatt Gas-Cooled Reactor (PC-MGCR) for Deep Space Exploration. *Ann. Nucl. Energy* **2025**, *221*, 110946.
29. Morales, A. A.; Pfeiffer, H.; Delfin, A.; et al. Phase Transformations on Lithium Silicates Under Irradiation. *Mater. Lett.* **2001**, *50*, 36–40.
30. Tang, T.; Zhang, Z.; Meng, J.-B.; et al. Synthesis and Characterization of Lithium Silicate Powders. *Fusion Eng. Des.* **2009**, *82*(12), 2124–2130.
31. Carella, E.; Hernández, T. Ceramics for Fusion Reactors: The Role of the Lithium Orthosilicate as Breeder. *Phys. B* **2012**, *407*, 4431–4435.
32. Cruz, D.; Bulbulian, S.; Lima, E.; et al. Kinetic Analysis of the Thermal Stability of Lithium Silicates ($Li_4SiO_4$ and $Li_2SiO_3$). *J. Solid State Chem.* **2006**, *179*(3), 909–916.
33. Che Zainul Bahri, C. N. A.; Mohd Al-Areqi, W.; Mohd Ruf, M. I. F.; et al. Characteristic of Molten Fluoride Salt System LiF–$BeF_2$ (FLiBe) and LiF–NaF–KF (Flinak) as Coolant and Fuel Carrier in Molten Salt Reactor (MSR). *AIP Conf. Proc.* **2017**, *1799*, 040008.
34. Cadwallader, L. C.; Longhurst, G. R. Flibe Use in Fusion Reactors: An Initial Safety Assessment. INEEL/EXT-99-00331, 1 April 1999. [CrossRef]
35. Williams, D. F.; Toth, L. M.; Clarno, K. T. Assessment of Candidate Molten Salt Coolants for the Advanced High-Temperature Reactor (AHTR). ORNL/TM-2006/12, 24 March 2006. [CrossRef]
36. Wu, Y. Neutronics Design Principles of Fusion–Fission Hybrid Reactors. In *Fusion Neutronics*; Wu, Y., Ed.; Springer: Berlin, Germany, 2017; pp. 283–308.
37. García Gallardo, J. A.; Giménez, M. A. N.; Gervasoni, J. L. Nuclear Properties of Tungsten Under 14 MeV Neutron Irradiation for Fusion–Fission Hybrid Reactors. *Ann. Nucl. Energy* **2020**, *147*, 107739.
38. Nukulin, V. Y.; Polukhin, S. N. Saturation of the Neutron Yield from Megajoule Plasma Focus. *Plasma Phys. Rep.* **2007**, *33*(4), 271–277.
39. Karami, F.; Rosham, M. V.; Habibi, M.; et al. Neutron Yield Scaling with Inductance in Plasma Focus. *IEEE Trans. Plasma Sci.* **2015**, *43*(7), 2155–2159.
40. Frignani, M.; Mannucci, S.; Mostacci, D.; et al. Short Circuit Tests on a 150 kJ, 1 Hz Repetitive Plasma Focus. *Czech. J. Phys.* **2006**, *56*, B413–B418.
41. Brovchenko, M.; Kloosterman, J. L.; Luzzi, L.; et al. Neutronic Benchmark of the Molten Salt Fast Reactor in the Frame of the EVOL and MARS Collaborative Projects. *Nucl. Sci. Technol.* **2019**, *5*, 2.
42. Kirsch, L. E.; Devlin, M.; Mosby, S. M.; et al. A New Measurement of the $^6$Li(n, $\alpha$)t Cross Section at MeV Energies

Using $^{252}$Cf Fission Chamber and $^{6}$Li Scintillators. *Nucl. Instrum. Methods Phys. Res. A* **2017**, *874*, 57–65.
43. Carlson, A. D.; Pronyayev, V. G.; Capote, R.; et al. Evaluation of the Neutron Data Standards. *Nucl. Data Sheets* **2018**, *148*, 143–188.
44. Brown, F.; James, R. H.; Perkin, J. L.; et al. The Cross Section of the $^{7}$Li(n, t) Reaction for Neutron Energies Between 3.5 and 15 MeV. *J. Nucl. Energy Part A/B* **1963**, *17*, 137–141.
45. Liskien, H.; Paulsen, A. Determination of $^{7}$Li(n, t) Cross Sections Between 6 and 10 MeV. *Ann. Nucl. Energy* **1981**, *8*, 423–429.
46. Smith, D. L.; Bretscher, M. M.; Meadows, J. W. Measurement of the Cross Section for the $^{7}$Li(n, n't)$^{4}$He Reaction in the 7– to 9–MeV Energy Range. *Nucl. Sci. Eng.* **1981**, *78*, 359–369.